



## Solvatochromism and potentiometric studies of some active nitroso- and nitroso-azo- compounds

Mamdouh Saad Masoud<sup>a,\*</sup>, Ekram Abd El-Moniem Khalil<sup>a</sup>,  
Saeda Abou El-Thana Abou El Enein<sup>b</sup> and Hesham Mostafa Kamel<sup>a</sup>

<sup>a</sup> Chemistry Department, Faculty of Science, Alexandria University, Alexandria, 21547, Egypt

<sup>b</sup> Chemistry Department, Faculty of Science, Minufiya University, Shebin El-Kom, 32511, Egypt

\*Corresponding author at: Chemistry Department, Faculty of Science, Alexandria University, Alexandria, 21547, Egypt. Tel.: +203.5832215; fax: +203.3911794.  
E-mail address: [drmsmasoud@yahoo.com](mailto:drmsmasoud@yahoo.com) (M. S. Masoud).

### REVIEW INFORMATION

Received: 16 February 2011  
Received in revised form: 20 March 2011  
Accepted: 16 April 2011  
Online: 30 September 2011

### KEYWORDS

Nitroso  
Pyridin-6-ylazo  
Triazine  
Effect of solvents  
Potentiometry  
Spectrophotometry

### ABSTRACT

The stability studies of biologically active 2,4-dinitrosoresorcinol, o-carboxy phenylazo-dinitrosoresorcinol, *N,N*-bis-[4,4'-(1,3-diphenyltriazine)]-diacetamide, 2-amino-6-phenylazo-pyridin-3-ol, 2-amino-3-hydroxy-pyridin-6-ylazo-benzoic acid, 4-(2-amino-3-hydroxy-pyridin-6-ylazo)-benzoic acid ethyl ester and *N*-[4-(2-amino-3-hydroxy-pyridin-6-ylazo)-phenyl]-acetamide compounds were studied. The dissociation constants were determined potentiometrically. The thermodynamic parameters of dissociation were evaluated. Regression analysis is applied for correlating the different parameters. The results help to assign the solute-solvent interactions and the solvatochromic potential of the investigated compounds. The electronic character of the substituent and the chemical nature of the solvent are major factors for the observed solvatochromism.

### 1. Introduction

Nitroso compounds are biologically active and have antibacterial and antiviral properties, have been extensively used as analytical reagents and are of potential importance to environment. These molecules have fundamental roles in processes such as catalysis, interaction of drugs with biomolecules and uptake of ions by living organism's [1-8]. Moreover, certain pyrimidine-pyrazoles have been studied in the fight against cancer [9-17]. In our laboratory, Masoud *et al.* recently reported a detailed structural chemistry of azo and nitroso metal complexes [18-26] based on spectral and magnetic susceptibility measurements. The following paper aimed to study the stability of biologically active nitroso and nitroso- azo compounds (Scheme 1).

### 2. Experimental

#### 2.1. Materials and solutions

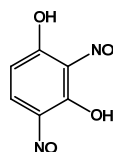
Organic solvents included 1, 4-dioxane, ethyl acetate, acetone, acetonitrile, 2-propanol, ethanol and methanol were used. An accurate CO<sub>2</sub>-free 0.01 M solution of KOH was prepared by diluting standard 1.0 M solution. The exact concentration of KOH was determined by titrating against standard potassium hydrogen phthalate. The solution was preserved in a waxed bottle fitted with a CaCl<sub>2</sub> tube.

1x10<sup>-2</sup>, 1x10<sup>-3</sup> mol L<sup>-1</sup> Stock ligand solutions were prepared by dissolving the required weight in the proper solvent for solubility (ethanol and dioxane). More dilute solutions were prepared by diluting the stock.

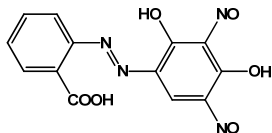
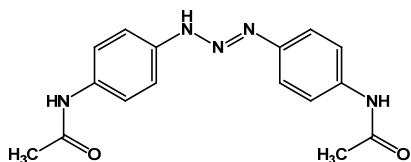
0.01 M Stock solutions of the metal salts (Co(II), Ni(II) and Cu(II)) were prepared by dissolving the exact amount of metal salts in appropriate volume of distilled H<sub>2</sub>O. The exact concentration was determined by complexometric titration against standard 0.01 M EDTA solution using the proper indicator for each ion.

#### 2.2. Potentiometric titration measurements

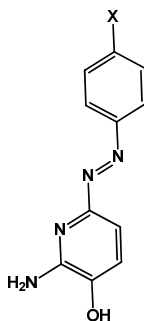
A Cole-Parmer instrument Company Model 60648 pH was used. The electrode system was calibrated before and after each series of pH measurements under the same conditions using standard buffers of pH 4.00 and 7.02. The titration cell consisted of 150 mL water jacketed vessel sealed with a polyethylene stopper in which appropriately located holes are present, one of them allowed the insertion of a 4 mL microburette accurate to 0.02 mL. The burette was filled by gentle suction exerted by a water pump and the KOH was protected from the atmospheric CO<sub>2</sub> by a tube containing CaCl<sub>2</sub>. Another hole was used to insert the combined electrode. The titrations were recorded under purified nitrogen gas atmosphere. This procedure was applied to evaluate the dissociation constants of the organic compounds by introducing the appropriate volume of the organic compound into the titration cell in presence of 5 mL 0.5 M KCl solution and different percentages mol.L<sup>-1</sup> of ethanol+water and dioxane+water media. It was left for about 15 min to attain the desired constant temperature controlled by using a thermostatic Techne Model U10 and titrating against standard KOH. During the whole titration, purified nitrogen gas was slowly bubbled in the solution. The same experimental setup was applied for studying the complex equilibria.



DNR = 2, 4 dinitroso resorcinol

DNRC = *o*-Carboxy azo-dinitroso resorcinol

NBDTD = N, N'-Bis-[4, 4'-(1, 3-diphenyl triazine)]-diacetamide



APP; X= H, COOH, NHCOCH<sub>3</sub>, COOC<sub>2</sub>H<sub>5</sub>  
 APP = 2-Amino-6-phenylazo-Pyridin-3-ol  
 AHPBA = 2-Amino-3-hydroxy-pyridin-6-ylazo)-benzoic acid  
 AHPA = N-[4-(2-Amino-3-hydroxy-pyridin-6-ylazo)-phenyl]-acetamide  
 AHPBAEE = 4-(2-Amino-3-hydroxy-pyridin-6-ylazo)-benzoic acid ethyl ester

Scheme 1

### 3. Results and discussion

#### 3.1. Effect of solvents on the electronic absorption spectra

It is known that UV-visible absorption spectra of chemical compounds may be influenced by surrounding medium where the solvents can bring about a change in position, intensity and shape of absorption bands [27]. The lack of reliable theoretical calculations of solvent effects in the past, and the inadequacy of defining "solvent polarity" in terms of simple physical solvent constants, have stimulated attempts to introduce empirical scales of solvent polarity, based on convenient, well-known, easily measurable, solvent-sensitive reference processes [28]. In order to predict spectral changes, it is necessary to find a set of physical parameters of the solvent-solute system that can be utilized in a predictive manner. Among the mechanisms proposed for interaction of solvent and solute molecules are hydrogen bonding, electromagnetic interaction between the dipole moments of solute and polar solvent [29]. Generally, the effect of solvents on the absorption bands of the substance consists in displacements and does not involve a fundamental change of the general form of the spectrum. In a sequel of continuation [30-33], the UV-vis spectra of DNR, NBDTD and DNRC (Scheme 1) were examined in various solvents. The

solvents were selected to show a wide variety of solvent parameters such as dielectric constant,  $D$ , refractive index,  $n$ , and hydrogen bonding capacity to permit a good understanding of solvent-induced spectral shifts. Different one-, two- and three-parameter equations are applied using suitable combinations between the solvent polarity parameters  $E$ ,  $K$ ,  $M$ ,  $J$ ,  $H$  and  $N$ .

$$E = 2.895 \times 10^{-3} \nu_{\max} \quad (1)$$

$$K = \frac{D-1}{2D+1} \quad (2)$$

$$H = \frac{n^2 - 1}{n^2 + 2} \quad (3)$$

$$J = \frac{D-1}{D+2} \quad (4)$$

$$M = \frac{n^2 - 1}{2n^2 + 1} \quad (5)$$

$$N = J - H \quad (6)$$

The parameter  $E$  is calculated from the wave number of the longest wavelength electronic transition of the negatively solvatochromic pyridinium *N*-phenolate betaine dye as probe molecule and is sensitive to both solvent-solute hydrogen bonding and dipolar interactions [28]. The dielectric function,  $K$ , of Kirkwood adequately represents the dipolar interactions and is related to the dielectric constant ( $D$ ) of the solvent [34]. The functions  $H$  and  $J$  have been introduced to account for the non-specific solute-solvent interactions such as dispersion and dipolar effects [35]. These are related to the dielectric constant ( $D$ ) and the refractive index ( $n$ ) of the solvents, respectively. The functions  $M$  and  $N$  account for the solute permanent dipole-solvent induced dipole and solute permanent dipole-solvent permanent dipole interactions, respectively [36]. Table 1 collects the values of these solvent parameters [37].

When a solute molecule with a permanent dipole is dissolved, both the electron distribution and the dipole distribution of the solvent molecules will be polarized to interact favorably with the solute molecules. On excitation, the direction and magnitude of the solute dipole change and consequently, the electronic distribution of the solvent will immediately respond to stabilize the new dipole. The electronic absorption spectra of the investigated compounds are collected in Table 2.

The observed peak position of an absorption band  $Y$  of any of the investigated compounds in a given solvent has been expressed as a linear function of different solvent polarity parameters  $X_n$ , as follows:

$$Y = a_0 + a_1X_1 + a_2X_2 + \dots + a_nX_n \quad (7)$$

where  $a_0$  is the regression intercept. It has been assumed [38] to be an estimate of the peak position for gas phase spectra and  $a_1, a_2, \dots, a_n$  are the solvent polarity parameters coefficients. From the last equation, it is possible to solution by multiple regression technique to correlate the observed spectral shifts with these empirical solvent polarity parameters. A program of statistical package of social sciences (SPSS) was used. Tables 3-5 show the results of regression analysis for some electronic transition peaks of the investigated compounds. The multiple correlation coefficients ( $R$ ) or (MCC) and the probability of variation ( $P$ ) have been considered as a measure of the fit.

**Table 1.** Solvent parameters used in the spectral correlation equations.

Solvent	n	D	E	K	H	J	M	N
1,4-dioxane	1.422	2.2	36.0	0.223	0.254	0.286	0.203	0.031
Ethyl Acetate	1.372	6.0	38.1	0.385	0.228	0.625	0.185	0.398
Acetone	1.359	20.7	42.2	0.465	0.220	0.868	0.180	0.648
Acetonitrile	1.344	37.5	46.0	0.480	0.212	0.924	0.175	0.712
2-Propanol	1.377	18.3	48.6	0.460	0.230	0.852	0.187	0.622
Ethanol	1.361	24.3	51.9	0.470	0.221	0.886	0.181	0.665
Methanol	1.329	32.6	55.5	0.477	0.203	0.913	0.169	0.710
Water	1.333	78.5	63.1	0.491	0.206	0.963	0.171	0.757

**Table 2.** The observed  $\lambda_{\max}$  values of the compounds [\* =  $Y_1$ ; \*\* =  $Y_2$ ].

R	1,4-dioxane	Ethyl Acetate	Acetone	Acetonitrile	2-Propanol	Ethanol	Methanol	Water
DNR	291.3*	243.6	327.3*	291.9*	291.5*	256.5	292.2*	302.4*
	442.8**	291.6*	442.8**	443.1**	443.1**	292.5*	436.8**	443.1**
	475.8	443.1**		476.1		442.8**		
DNRC	290.7	330.3	332.4	269.1	329.4	331.1	257.1	321.3
	442.8	436.8		316.5	442.8		324.0	442.8
				333.9	657.0		436.5	
NBDDT	220	248	360**	226	294*	204	232	287*
	288*	284*		286*	370**	222	292*	369**
	368**	368**		364**		292*	370**	
						370**		

**Table 3.** Regression analysis data for the high-energy transition  $Y_1$  and  $Y_2$  bands of compound DNR.

Parameters	$Y_1$				P	MCC
	$a_0$	$a_1$	$a_2$	$a_3$		
K	282.042	35.943			0.068	0.532
M	356.170	-321.000			0.070	0.527
N	290.262	12.879			0.062	0.551
E	299.026	-0.003			0.001	0.959
K,M	323.542	18.553	-186.184		0.076	0.821
K,N	263.892	119.411	-31.559		0.074	0.825
K,E	291.705	-0.546	73.815		0.149	0.669
M,N	338.065	-234.961	4.224		0.072	0.831
M,E	562.892	-1157.197	-1.135		0.270	0.455
N,E	311.971	32.381	-0.688		0.167	0.633
K,M,N	347.001	263.778	-565.211	-106.105	0.111	0.914
K,M,E	527.653	-1.139	20.415	-1011.532	0.277	0.696
M,N,E	525.863	-977.503	9.867	-1.164	0.279	0.693
K,N,E	376.307	132.661	-1.016	-244.498	0.193	0.812
K,M,N,E	539.760	-101.313	-919.179	52.763	-1.271	0.283

Parameters	$Y_2$				P	MCC
	$a_0$	$a_1$	$a_2$	$a_3$		
K	444.112	-4.422			0.034	0.662
M	423.950	100.000			0.224	0.236
N	443.274	-1.888			0.044	0.617
E	445.942	-0.079			0.106	0.430
K,M	397.026	15.309	211.248		0.355	0.334
K,N	435.244	36.362	-15.420		0.080	0.811
K,E	445.746	-0.092	1.981		0.110	0.747
M,N	393.148	246.380	7.187		0.384	0.298
M,E	413.519	142.193	0.057		0.241	0.502
N,E	446.260	0.794	0.095		0.110	0.748
K,M,N	391.825	-39.059	295.282	23.524	0.412	0.502
K,M,E	387.247	0.055	15.220	250.789	0.371	0.562
M,N,E	387.216	269.835	7.009	0.037	0.391	0.533
K,N,E	445.014	-1.147	-0.088	4.732	0.110	0.915
K,M,N,E	392.837	-40.976	293.424	24.358	-0.007	0.412

The observed changes in UV-vis spectra recorded for the investigated compounds in various solvents can be categorized as follows: (1) absorption peaks become broader which is called solvent broadening, (2) the position of  $\lambda_{\max}$  differs in different solvents from the solvatochromism; [38] which can be either positive solvatochromism in which the shift in the peak position is subjected to hypsochromic effect or blue shift or negative solvatochromism in which the shift is bathochromic or red shift, and (3) peak intensity may differ in different solvents to give either hyperchromic effect or hypochromic effect. Better stabilization of the molecule in the first excited state relative to that in the ground state with increasing solvent polarity, will lead to positive solvatochromism. In this context, the first Franck-Condon excited state with the solvation pattern presents in the ground state [39]. The observed solvatochromism depends on the chemical structure and

physical properties of the chromophore and the solvent molecules, which, for their part, determine the strength of the intermolecular solute/solvent interactions in the equilibrium ground state and the Franck-Condon excited state. The electronic spectra of the investigated compounds in different solvents are shown in Figure 1.

The spectral bands of DNR, NBDDT and DNRC in the UV-visible region are generally due to  $n \rightarrow \pi^*$  (B band),  $\pi \rightarrow \pi^*$  (K band), and charge transfer (R band), Table 2 and Figure 1. A strong band at the wavelength range 259-334 nm in most solvents used is mainly of the  $\pi\text{-}\pi^*$  type followed by a number of longer wavelength bands (up to ~360 nm). The longer wavelength side is mainly of the  $n\text{-}\pi^*$  type.

**Table 4.** Regression analysis data for the high-energy transition of DNRC.

Parameters	a <sub>0</sub>	a <sub>1</sub>	a <sub>2</sub>	a <sub>3</sub>	a <sub>4</sub>	P	MCC
K	347.262	-39.640				0.528	0.084
M	264.114	360.000				0.121	0.411
N	337.868	-13.867				0.434	0.127
E	350.726	-0.442				0.027	0.655
K,M	211.555	52.409	517.227			0.271	0.480
K,N	165.788	614.391	-187.775			0.347	0.411
K,E	324.726	-0.676	81.612			0.029	0.829
M,N	225.355	523.266	14.513			0.286	0.465
M,E	346.656	18.738	-0.428			0.118	0.656
N,E	347.816	25.785	-0.720			0.028	0.833
K,M,N	166.651	329.102	367.599	-87.085		0.478	0.517
K,M,E	276.185	-0.576	98.839	196.803		0.076	0.870
M,N,E	295.025	239.129	33.281	-0.621		0.060	0.890
K,N,E	352.785	31.149	-0.729	-17.332		0.110	0.833
K,M,N,E	347.550	-241.326	314.622	110.334	-0.706	0.172	0.910

**Table 5.** Regression analysis data for the high-energy transition Y<sub>1</sub> and Y<sub>2</sub> bands of compound of NBDTD.

Parameters	Y <sub>1</sub>				P	MCC
	a <sub>0</sub>	a <sub>1</sub>	a <sub>2</sub>	a <sub>3</sub>		
K	284.784	9.869			0.067	0.574
M	296.385	-40.385			0.015	0.795
N	286.865	3.832			0.073	0.558
E	282.368	0.137			0.124	0.438
K,M	263.639	18.795	94.792		0.094	0.821
K,N	291.493	-20.967	11.600		0.077	0.851
K,E	282.420	0.146	-1.115		0.125	0.766
M,N	256.807	147.746	9.290		0.123	0.770
M,E	208.012	318.538	0.469		0.310	0.476
N,E	281.886	-0.903	0.157		0.126	0.765
K,M,N	254.100	-90.736	259.498	47.036	0.180	0.877
K,M,E	188.146	0.444	14.090	400.859	0.353	0.684
M,N,E	189.858	410.351	6.133	0.427	0.354	0.683
K,N,E	268.252	-22.027	0.234	50.803	0.140	0.915
K,M,N,E	189.897	-0.254	410.482	6.241	0.581	0.874

Parameters	Y <sub>2</sub>				P	MCC
	a <sub>0</sub>	a <sub>1</sub>	a <sub>2</sub>	a <sub>3</sub>		
K	368.913	-3.556			0.008	0.831
M	366.767	3.333			0.001	0.982
N	367.973	-1.052			0.005	0.866
E	359.805	0.159			0.162	0.322
K,M	384.528	-10.100	-70.057		0.021	0.947
K,N	378.831	-49.167	17.245		0.030	0.927
K,E	362.609	0.356	-28.266		0.430	0.246
M,N	382.709	-72.429	-3.720		0.016	0.960
M,E	267.322	405.590	0.546		0.569	0.122
N,E	354.572	-13.091	0.425		0.498	0.179
K,M,N	381.182	-45.085	-15.983	15.137	0.030	0.987
K,M,E	286.302	0.548	-10.996	327.133	0.595	0.263
M,N,E	291.560	287.970	-6.459	0.565	0.617	0.237
K,N,E	302.425	-94.371	0.690	198.173	0.706	0.145
K,M,N,E	268.458	168.417	191.015	-77.767	0.743	0.260

The two lone pairs of electrons of the azo group in DNRC and NBDTD are not the only interacting non-bonding electrons, since aryl group part of the molecules contains different substituents containing nitrogen and oxygen atoms. Thus, other  $n-\pi^*$  transitions are expected to take place from these non-bonding orbitals to different  $\pi^*$  molecular orbitals. The extra  $\pi-\pi^*$  transition at 204-257 nm in hydrogen bonding solvents (e.g. ethanol, methanol and H<sub>2</sub>O) is due to the presence of an external hydrogen bond affecting the K band [40]. The slight shift of  $\lambda_{\max}$  of the electronic spectral bands from alcohol (EtOH or MeOH) to H<sub>2</sub>O, Table 2, depicts the presence of an internal hydrogen bond [41], affected by the interaction with n-electrons blocked by the solvent leading to an increased localization of electrons. The delocalized 2p orbital with the neighbouring atom will necessarily be the one involved in bonding to the solvents.

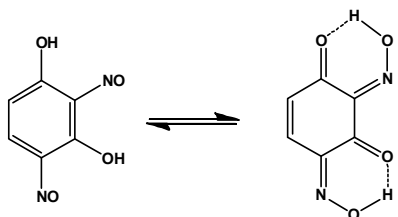
DNR exhibits absorption maxima at the wavelengths of 243.6 and 476.4 nm that make it efficient chromophore although its color strength does not reach that of molecules having azo chromophores [42,43]. This absorption band is assigned to the partly forbidden ( $n\rightarrow\pi^*$ ) transition. This band shows positive solvatochromism upon increasing solvent

polarity. This behavior is accounted as those molecules in the ground state are less polar than those in the excitation. This leads to a simplification of assumptions that DNRC with non-polarized ground state are strongly polarized in protic solvents, because the high-energy, polar structure of the excitation state is stabilized. The excited state energy is lowered and the ground state is not significantly affected. The energy difference between ground and excited states is decreased so the excitation energy is decreased.

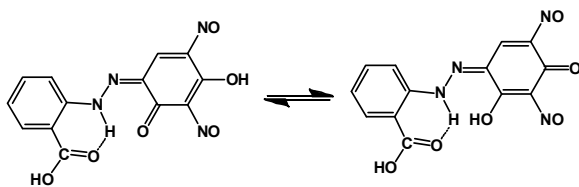
The approximation of the energy levels expresses itself in a bathochromic shift of the spectrum with increasing polarity of the solvent. A negative solvatochromism is noticed in solvents like ethyl acetate. This dipolar aprotic solvent destabilizes the polarized electronic state leading to a hypsochromic shifting. For DNRC with an electron withdrawing group on the azo benzene nucleus, solvatochromism is observed in the ( $n\rightarrow\pi^*$ ) absorption upon increasing the electron withdrawing character of the substituents [44]. The lowest transition absorption band is assigned to ( $n\rightarrow\pi^*$ ) transition while the other absorption band corresponding to the higher energy is assigned as ( $\pi\rightarrow\sigma^*$ ) transition. The high-energy band shows a positive solvatochromism in all solvents. The degree of the

solvatochromic behavior is increased upon increasing the solvent polarity. The ( $n \rightarrow \pi^*$ ) band shows a negative solvatochromism in all solvents. The spectral shifts decrease with gradual introduction of the more polar solvent. In presence of dipolar aprotic media such as ethyl acetate that act as proton acceptor in hydrogen bond formation with the acidic COOH group of the DNRC. However, these solvents have relatively high dipole moments. The dipole-dipole interactions with the solute molecules especially in their excited states will account for the blue shifts observed in these solvents. The energy of a charge transfer will increase as the strength of such hydrogen bonds increases. The observed marginal shift in the absorption maximum for the azo dyes may include other contributors than the ones created by the solvent. However, in addition to these shifts, a significant band broadening for the azo compounds with increasing solvent polarity was observed. It is concluded that solvatochromism is a useful indicator of the strength of hydrogen bonds and has been a good tool to assess their strengths. The blue shift for this band follows the order  $\text{OH} > \text{COOH}$ , in the opposite direction of inductive effect, because the involvement of the carboxylic group in intermolecular hydrogen bonding is more than that of the hydroxyl group.

DNRC and NBDTD seem to exist in their *trans* azo isomer form which possesses a lower steric instability than the *cis* isomer [45] and the following intramolecularly hydrogen bonded structures are expected to be the most stable (Scheme 2 and 3).



Scheme 2



Scheme 3

The presence of an internal hydrogen bond is also suggested by the low degree of association of the investigated compounds in organic solvents. Such compounds could be represented as resonance hybrid, i.e. should contain a non-localized bond. This leads to the displacement of the B- and K-bands to longer wavelengths, because the polarity of the absorbing system (in its ground state) is increased by polarization. However, the effect of an internal hydrogen bond on R-bands is in contrast of B- and K-bands. So, the presence of an internal hydrogen [46] bond was supported by the characteristic blue shift of its maximum in ethanol and water, respectively [47].

Only a negative solvatochromism is observed for all substituents using solvents which have the ability to form hydrogen bonding with the solute molecules, like 2-propanol, ethanol, methanol and water. It seems like when there is strong hydrogen bonding the push-pull effect is retarded. The opposite trend in the solvatochromic behavior of ( $n \rightarrow \pi^*$ ) absorption for these compounds is observed in solvents like ethyl acetate. The electronic absorption spectra of the (DNR in dioxane and acetonitrile), (NBDTD in ethyl acetate, acetonitrile,

dioxane and methanol) and (DNRC in acetonitrile, 2-propanol and methanol) exhibit three absorption bands, while the electronic absorption spectra of the (DNR in ethyl acetate and ethanol) and (NBDTD in ethanol) exhibit four absorption bands. The band at higher wavelengths is assigned to ( $n \rightarrow \pi^*$ ) transition that is red shifted in all other solvents. The same behavior was found for the second absorption band which assigned as ( $\pi \rightarrow \sigma^*$ ). A third band appeared in the spectrum is due to localized aromatic rings of ( $\pi \rightarrow \pi^*$ ) transition and shows a negative solvatochromism in all other solvents. Several one-, two- and three-parameter equations have been used to correlate the spectral shifts with various empirical solvent polarity parameters using the multiple linear regression technique. Each of the solvent parameters used has a fixed relative sensitivity to each of the various interaction mechanisms. The multiple correlation coefficients, MCC have been used in a one-tail test to obtain the level of significance for each test. The high value of MCC (near one) means that a certain solvent parameter has a good correlation to the spectral shifts. In other words, the spectral shifts for the peak are greatly sensitive to the solvent parameter that gives a value of MCC near to unity. Alternatively, the small value (near zero) of the significance parameter (P) means the correlation is good. The analysis of the spectral shifts of the high-energy transitions in all of the investigated compounds using one-parameter equation showed that the relatively best MCC value is obtained for the parameter M in case of NBDTD ( $Y_2$ ) which is sensitive to dipole-dipole interactions.

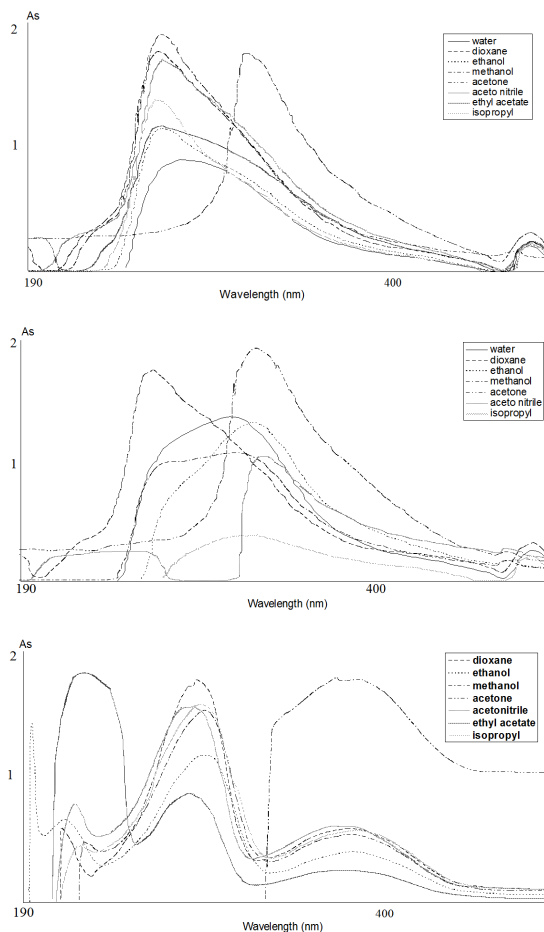


Figure 1. Effect of solvents on the electronic absorption spectra of DNR, DNRC and NBDTD.



**Table 6.**  $\nu_{(\text{vapour})}$ ,  $K_1$ ,  $K_2$  and the correlation analysis data for the ligands.

Ligand	$\nu_{(\text{vapour})} \text{ cm}^{-1}$	$K_1$	$K_2$	Variables	P	MCC
DNR ( $X_1=0$ )	25294	-----	5574.6	$X_1$	0.111	0.421
DNR ( $X_2=0$ )	28756	-1740.6	-----	$X_2$	0.431	0.077
				$X_1, X_2$	0.731	0.038
DNRC ( $X_1=0$ )	26631	-----	4296.1	$X_1$	0.044	0.616
DNRC ( $X_2=0$ )	28353	-198.17	-----	$X_2$	0.096	0.454
				$X_1, X_2$	0.117	0.733
NBDTD ( $X_1=0$ )	32651	-----	-13488	$X_1$	0.374	0.107
NBDTD ( $X_2=0$ )	26237	1802.9	-----	$X_2$	0.283	0.175
				$X_1, X_2$	0.374	0.310

The respective MCC value is 0.982 indicating that the solvatochromism for these cases can be interpreted in terms of solute permanent dipole-solvent permanent dipole interactions. The parameters [E (0.959)( $Y_1$ ) and K (0.662)( $Y_2$ )] in case of DNR, [M (0.411) and E (0.655)] in case of DNRC and M (0.795)( $Y_1$ ) in case of NBDTD gave the best correlations to the solvent-induced spectral shifts for the high-energy electronic transitions among all of the other parameters. This means that the solute permanent dipole-solvent induced dipole interactions and the dipolar interactions are the major factors affecting the solvatochromism in these cases, respectively. However, the parameter E gives a moderate correlation [MCC = 0.001] for DNRC, i.e. the intermolecular hydrogen bonding with the solvent is the effective parameter to explain the spectral shifts rather than the other parameters. This is probably due to the presence of the COOH group in the ortho position, which facilitates the formation of hydrogen bonds with the solvent. The correlation of the two-parameter equations with the solvent spectral shifts was also studied and gave, as expected, better fit to these spectral shifts than the corresponding one-parameter fits. Solvent's ability to form hydrogen bonds with solute molecules, which is reflected by the parameter E when combined with the previously mentioned parameters K, M or N is the reason for improving the correlations. For instance, when the parameter E is combined with the parameters [E ( $Y_1$ ) and N ( $Y_2$ )] (DNR) and E (DNRC) the MCC values jumped to [0.959 and 0.617] and 0.655, respectively. The correlation is improved as expected on analyzing the spectral shifts using three-parameter equations and the best MCC values are observed. The best MCC value is obtained for the parameter K (0.831) ( $Y_2$ ) in case of NBDTD. This means the solvatochromic behavior for this transition in NBDTD is mainly controlled by the solvent's ability to form hydrogen bonding with the solute molecules. Form the values of MCC for the rest of the compounds; it is clear that one solvent parameter can not interpret the solvatochromic behaviour for this electronic transition alone. The correlation is improved as expected on analyzing these spectral shifts using two- and three-parameter equations. It was concluded that the parameters N, E and K are the major parameters affecting the solvatochromism when used in combinations. Thus solute permanent dipole-solvent permanent dipole interactions combined with the solvent's hydrogen bonding capacity and/or dipolar interaction are contributing mainly to the observed solvatochromism. Different combinations of the K, M, N parameters gave the best correlations. This means that in addition to K and N, the parameter M, which is related to the solvent refractive index and accounts for the solute permanent dipole-solvent induced dipole interactions should be involved in the interpretation of the observed solvatochromism. Thus, the determination of the solvent spectral shifts is controlled mainly by the dipolar interactions as well as both the solvent dielectric constant and the solvent refractive index. Generally, it was concluded that the addition of a third solvent parameter to the two-parameter equations always gave rise to improvements in the correlation with the solvent induced spectral shifts. In most cases, the

different three-parameter combinations have been selected on the basis of the results of the two-parameter combinations discussed before. In a test for the significance of a one-tail test, the level of significance for all these different three-parameter combinations was found to be above 90%. This indicated that specific solute-solvent interactions in particular hydrogen bonding and non-specific solute-solvent interactions such as dispersion and dipolar effects had provided a reasonable model for describing the solvent induced spectral shifts in a predictive manner.

According to  $N = J - H$  a two - parameter equation was also applied [42]

$$\nu_{(\text{solution})} = \nu_{(\text{vapour})} + K_1 \left( \frac{2D-2}{2D+2} \right) + K_2 \left( \frac{2n^2-2}{2n^2+1} \right) \quad (8)$$

$$X_1 = \left( \frac{2D-2}{2D+2} \right) \quad (9)$$

$$X_2 = \left( \frac{2n^2-2}{2n^2+1} \right) \quad (10)$$

where  $\nu_{(\text{solution})}$  is the frequency of the peak maximum in presence of solvents; D, dielectric constant; n, refractive index; and  $\nu_{(\text{vapour})}$ , frequency of the peak maximum in absence of solvents.

Multiple regression technique was used in order to evaluate  $\nu_{(\text{vapour})}$ ,  $K_1$ ,  $K_2$  and the correlation coefficients. The results are listed in Table 6.

On plotting  $\nu_{(\text{solution})}$  vs.  $X_1$  or  $X_2$ , Figure 2, the coefficients  $K_1$  and  $K_2$  and intercept  $\nu_{(\text{vapour})}$  were calculated for each peak by using the procedure described above. The data in general point that both the dielectric constant and the refractive index of solvents affect the electronic spectral properties of the compounds, but with different degrees. The negative values of  $K_1$  and  $K_2$  indicate strong solute - solvent interaction, and causing decrease in energy of electronic transition from LUMO to HOMO compared with the vapor state. In each case, fits were obtained as a function of  $X_1$  alone,  $X_2$  alone, and both  $X_1$  and  $X_2$ . As an indication of the fit, the sum of the squared residuals was calculated for each.

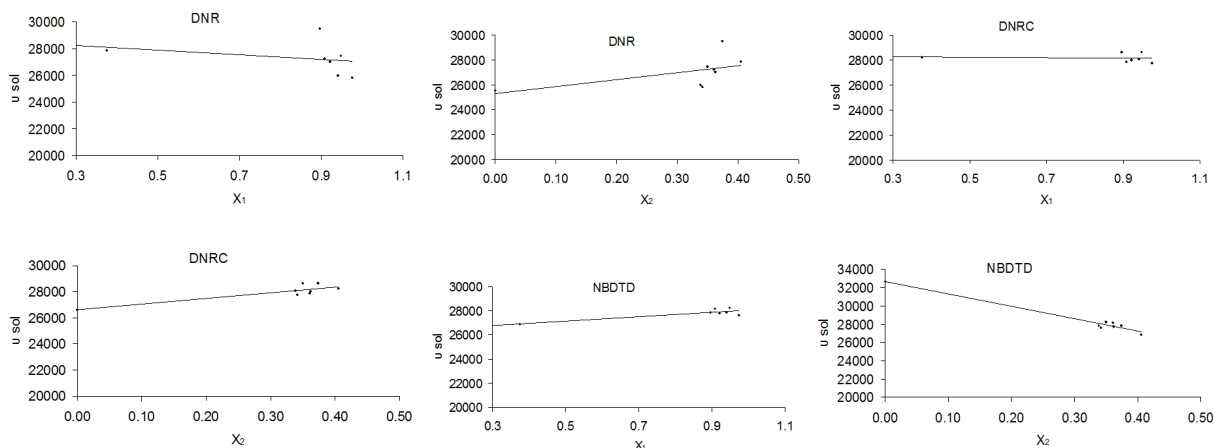
The data show strong dependence of the shift in  $\lambda_{\text{max}}$  [DNR on  $X_1$ , DNRC on ( $X_1, X_2$ ) and NBDTD on ( $X_1, X_2$ )], Table 6. This is inferred from the high positive values of MCC (multiple correlation coefficients) in case of DNRC. The MCC coefficients are in good agreement for the DNRC and NBDTD compounds. However, certain coefficients are poor for DNR compound.

### 3.2. Potentiometric titration studies

Acidity and stability constants were determined by using acid-base titration techniques of the free ligands: 2,4-dinitrosorsorsinol (DNR), *o*-carboxyazo-dinitroso resorsinol (DNRC), *N,N'*-bis-[4,4'-(1,3-diphenyl triazine)]-diacetamide

**Table 7.** pK values for the compounds in ethanol+water and dioxane+water at different temperatures\*.

% of Solvents	Compound	$\bar{n}_A$ -pH				Point-wise method				Algebraic method			
		25 °C	30 °C	35 °C	40 °C	25 °C	30 °C	35 °C	40 °C	25 °C	30 °C	35 °C	40 °C
25% Ethanol+water	DNR	7.24 (10.87)	7.49 (10.83)	6.93 (10.60)	6.97 (10.65)	7.25 (10.81)	7.51 (10.81)	6.90 (10.55)	7.04 (10.63)	7.23 (10.85)	7.50 (10.81)	6.91 (10.57)	7.05 (10.65)
	AHPBA	10.41	10.47	10.40	10.42	10.42	10.51	10.36	10.31	10.42	10.50	10.38	10.40
	AHPA	10.38	10.36	10.32	10.42	10.43	10.40	10.36	10.48	10.40	10.40	10.34	10.45
	NBDTD	10.78	10.84	9.94	10.51	10.75	10.80	9.95	10.5	10.72	10.81	9.93	10.53
	APP	10.87	10.75	10.40	9.44	10.80	10.69	10.36	9.40	10.85	10.70	10.38	9.42
50% Ethanol+water	DNR	7.06 (10.34)	7.09 (10.41)	7.30 (10.65)	6.95 (10.00)	7.03 (10.30)	7.08 (10.35)	7.25 (10.60)	6.86 (9.92)	7.05 (10.35)	7.10 (10.37)	7.27 (10.63)	6.90 (9.95)
	AHPBA	6.16	5.82	5.68	---	6.36	5.96	5.77	---	6.20	5.90	5.70	---
	AHPA	---	10.49	10.23	10.11	---	10.61	10.30	10.14	---	10.50	10.25	10.13
	AHPBAEE	10.06	9.81	9.76	9.09	10.09	9.82	9.75	9.09	10.08	9.82	9.77	9.10
	NBDTD	10.59	11.07	10.86	10.81	10.59	11.04	10.86	10.79	10.57	11.05	10.83	10.80
75% Ethanol+water	APP	11.15	11.06	10.97	10.41	11.11	11.04	10.94	10.35	11.13	11.09	10.95	10.40
	DNR	8.06 (11.12)	6.02 (11.17)	7.17 (9.30)	6.42 (11.03)	8.02 (11.05)	6.10 (11.05)	7.10 (9.20)	6.47 (10.95)	8.06 (11.07)	6.08 (11.12)	7.12 (9.30)	6.45 (11.00)
	AHPBA	11.23	11.43	---	---	11.25	11.46	---	---	11.25	11.47	---	---
	AHPA	10.52	10.90	---	---	11.13	11.45	---	---	10.80	11.00	---	---
	NBDTD	11.58	11.45	11.25	11.25	11.58	11.42	11.23	11.23	11.55	11.46	11.21	11.21
APP	11.56	11.43	11.24	11.04	11.55	11.41	11.24	11.02	11.57	11.43	11.25	11.03	
25% Dioxane+water	DNR	6.46 (10.00)	6.02 (10.48)	6.23 (10.44)	6.26 (10.36)	6.46 (9.96)	5.78 (10.42)	6.00 (10.37)	5.90 (10.27)	6.47 (9.98)	5.92 (10.45)	6.11 (10.40)	6.00 (10.30)
	DNRC	6.39 (8.26)	5.6 (8.17)	5.99 (8.18)	6.13 (8.21)	6.35 (8.24)	5.58 (8.15)	5.91 (8.17)	6.07 (8.19)	6.36 (8.25)	5.60 (8.16)	5.95 (8.17)	6.10 (8.20)
	AHPBA	7.61 (10.60)	6.24 (10.12)	5.94 (9.22)	5.47 (9.19)	7.63 (10.60)	6.49 (10.05)	6.00 (9.29)	5.70 (9.20)	7.62 (10.61)	6.40 (10.08)	5.98 (9.25)	5.60 (9.20)
	AHPBAEE	10.48	10.63	10.55	10.35	10.46	10.63	10.54	10.32	10.47	10.64	10.55	11.34
	NBDTD	10.97	10.80	10.74	10.19	10.94	10.78	10.74	10.19	10.95	10.79	10.75	10.20
	APP	10.91	10.91	10.65	10.43	10.90	10.90	10.60	10.41	10.91	10.91	10.63	10.42
50% Dioxane+water	DNR	8.65 (11.65)	6.39 (10.95)	7.51 (10.65)	6.81 (10.65)	8.60 (11.68)	6.70 (10.90)	7.25 (10.60)	6.39 (10.62)	8.60 (11.65)	6.50 (10.92)	7.30 (10.65)	6.50 (10.62)
	DNRC	7.76 (8.91)	6.56 (8.43)	6.58 (8.14)	6.72 (8.26)	7.74 (8.93)	6.67 (8.40)	6.50 (8.10)	6.50 (8.28)	7.74 (8.91)	6.60 (8.41)	6.55 (8.12)	6.70 (8.26)
	AHPBA	7.56 (10.07)	6.67 (9.55)	6.59 (9.50)	6.52 (9.40)	7.60 (10.05)	6.67 (9.53)	6.58 (9.48)	6.52 (9.35)	7.58 (10.05)	6.67 (9.55)	6.57 (9.50)	6.53 (9.37)
	AHPA	---	8.49	8.26	8.78	---	8.80	8.27	8.50	---	8.50	8.26	8.61
	AHPBAEE	9.20	9.24	9.24	9.35	9.18	9.24	9.21	9.36	9.21	9.25	9.23	9.36
	NBDTD	11.34	11.23	11.17	11.03	11.35	11.25	11.15	11.00	11.35	11.24	11.17	11.02
APP	11.37	11.30	11.21	10.91	11.30	11.30	11.20	10.90	11.35	11.30	11.19	10.92	
75% Dioxane+water	DNR	8.15 (11.51)	7.83 (10.98)	8.45 (11.54)	---	8.00 (11.45)	7.70 (10.82)	8.38 (11.45)	---	8.10 (11.50)	7.75 (10.99)	8.40 (11.50)	---
	NBDTD	12.11	11.75	11.87	11.71	12.11	11.75	11.87	11.71	12.12	11.78	11.88	11.73
	APP	12.11	12.01	11.08	11.44	12.10	12.00	11.10	11.40	12.12	12.02	11.09	11.42

\* Values between brackets are pK<sub>2</sub>.**Figure 2.** Solvent Parameters-Relation  $\bar{n}_{\text{solution}}$  against  $X_1$  ( $X_2=0$ ) or  $X_2$  ( $X_1=0$ ) for the ligands.

(NBDTD), 2-amino-6-phenylazo-Pyridin-3-ol (APP), 2-amino-3-hydroxy-pyridin-6-ylazo)-benzoic acid (AHPBA), 4-(2-amino-3-hydroxy-pyridin-6-ylazo)-benzoic acid ethyl ester (AHPBAEE) and *N*-[4-(2-amino-3-hydroxy-pyridin-6-ylazo)-phenyl]-acetamide (AHPA) against standard KOH in presence of 0.5 M KCl. The application of the potentiometric measurements depends

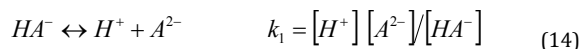
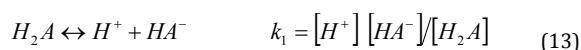
on the evaluation of the average number of the protons associated with the reagent,  $\bar{n}_A$  [48]. This was determined at different pH's using the simplified following equation [48]:

$$\bar{n}_A = Y - \frac{V_f N^o}{V_o C_L} \quad (11)$$

Where  $V_i$  denotes the volume of alkali required to reach a given pH on the titration curve,  $V_0$  is the initial volume of the ligand,  $N^0$  is the alkali concentration,  $C_L$  is the total concentration of the ligand and  $Y$  is the number of displaceable hydrogen atoms in the ligand. The dissociation constants are obtained by plotting  $\bar{n}_A$  against pH for the free ligands. Two pK's values were obtained for ligands with  $Y = 2$  [for DNR (all percentage of the two solvents), AHPBA {(25%, 50% dioxane+water) and (50% ethanol+water)} and DNRC] by recording the pH values at  $\bar{n}_A = 0.5$  and 1.5 (pK<sub>1</sub> and pK<sub>2</sub>, respectively). Only one pK value with  $Y = 1$  [for NBDTD, APP, AHPA (25, 50, 75% of ethanol+water and dioxane+water), AHPBAEE (25, 50, 75% of ethanol+water and 25, 50% dioxane+water) and AHPBA] by recording the pH at  $n = 0.5$  pK<sub>1</sub>. The data are collected in Table 7. The point-wise calculation [49] was used for the same purpose, where concordant results are obtained, Table 7.

$$pH = \log \frac{\bar{n}_A - 1}{2 - \bar{n}_A} + pK_1 \quad pH = \log \frac{\bar{n}_A}{1 - \bar{n}_A} + pK_2 \quad (12)$$

The plot of the  $\log \bar{n}_A$  ratio versus pH gives the required pK values, Table 7. A method reported by Martell *et al.* [50] was applied to calculate the dissociation constants of ligands where the equilibrium involved as follows:



$H_2A$  represents the ligands and parentheses represent the molar concentrations. Since  $K_1 > K_2$ , each dissociation stage was considered separately. If  $C_A$  represents the total concentration of the ligand species and "a" represents the number of moles of base added per mole of the ligand present. It follows that in the low pH buffer region:

$$C_A = [H_2A] + [HA^-] \quad (15)$$

$$aC_A + [H^+] = [HA^-] + [A^{2-}] \quad (16)$$

$$K_1 = \frac{[H^+][aC_A + [H^+]]}{C_A - (aC_A + [H^+])} \quad (17)$$

$$K_2 = \frac{[H^+](a-1)C_A - [OH^-]}{(2-a)C_A - [OH^-]} \quad (18)$$

In the high pH buffer region, the concentration of the acid from ( $H_2A$ ) of the ligand may be neglected and so, compounds in aqueous and different percentages of ethanol+water media and dioxane+water media gave two pK's values based on potentiometric measurements are due to two hydroxy groups ionization [51].

AHPBA, AHPBAEE, AHPA, NBDTD and APP compounds gave one pK value due to the carboxylic, hydroxyl, amino group's ionization. In the case of DNR and DNRC compounds in aqueous and different percentages of ethanol+water media and dioxane+water media gave two pK's values based on potentiometric measurements, due to the removal of a proton from the -OH groups [52,53].

The data obtained showed that, the pK values are dependent upon both the nature and the proportion of the organic co-solvent. In general, increasing the organic co-solvent

content in the medium results in an increase in the pK value. According to Coetzee and Ritchie [54], the acidity constants in a pure aqueous medium ( $K_{a1}$ ) can be related to that in water-organic solvent mixtures ( $K_{a2}$ ) by the equation

$$K_{a1} = K_{a2} (\gamma_{H^+} \gamma_{A^-} / \gamma_{HA}) \quad (19)$$

where  $\gamma$  is the activity coefficient of the subscripted species in a partially aqueous medium to that in a pure aqueous one. Since it is known that the electrostatic effects of solvents operate only on the activity coefficients of charged species [55], the increase in the amount of the organic co-solvent in the medium will increase the activity coefficients of both  $H^+$  and  $A^-$  ions, this will result in a decrease in the acid dissociation constant (high pK value), which is consistent with the results obtained for the investigated compounds. Moreover, though ethanol and dioxane have comparable dielectric constants (24.3 and 2.21, respectively at 25 °C), all the compounds are more acidic in ethanol+water media than in dioxane+water media, where the same mole fraction of each mixture is used. This behaviour indicates that other solvent effects beside the electrostatic one have contribution in the ionization process of the investigated compounds.

The behaviour of the discussed compounds was investigated in the temperatures range 25-40 °C, where the  $\Delta G^\ddagger$ ,  $\Delta H^\ddagger$  and  $\Delta S^\ddagger$  values are evaluated, Table 8. The equation  $K = Ae^{-\Delta E/RT}$  is applied based on pK values. Plotting the pK values versus  $1/T$ , gave straight lines with a slope of  $\Delta H/2.3R$  from which  $\Delta H$  values (Kcalmol<sup>-1</sup>) are computed. The free energy values  $\Delta G$  (kcal.mol<sup>-1</sup>) are calculated using the equation  $\Delta G = 2.3RT$  pK. The  $\Delta S$  (e.v) values are calculated based on  $\Delta G^\ddagger = \Delta H^\ddagger - T\Delta S^\ddagger$ .

The intramolecular hydrogen bonding gives rise to + $\Delta S$  values whereas the hydrogen bonding to solvent leads to higher degree of solvent ordering with a - $\Delta S$  value [53,56]. The - $\Delta S$  values for the most compounds in different percentages of ethanol+water mixtures are attributed to the predominant presence of intermolecular hydrogen bonding.

The isokinetic temperature relation for the plot of  $\Delta H^\ddagger$  versus  $\Delta S^\ddagger$  for pK<sub>1</sub> and pK<sub>2</sub> for the investigated compounds gives a best fit straight line. Figure 3 is based on the relation  $\Delta H^\ddagger = \beta \Delta S^\ddagger$ , where the isokinetic temperature  $\beta$  value is obtained from the slope of the plot. The plot is of straight line relation and passes through the origin to satisfy the validity of this equation.

The effect of ethanol and dioxane on the behaviour of these compounds is discussed using another scope. We assume that the  $J$  factor represents a solvent-transfer number characteristic of the tested chemical reaction which can be attributed to the transfer of the solvent. The following equation [52] is tested:

$$J \log [S] - \log K = -\Delta G / (2.303 RT) - W \log [H_2O] / [S] + J \log [H_2O] \quad (20)$$

$$\log [H_2O] / [S] = X \quad (21)$$

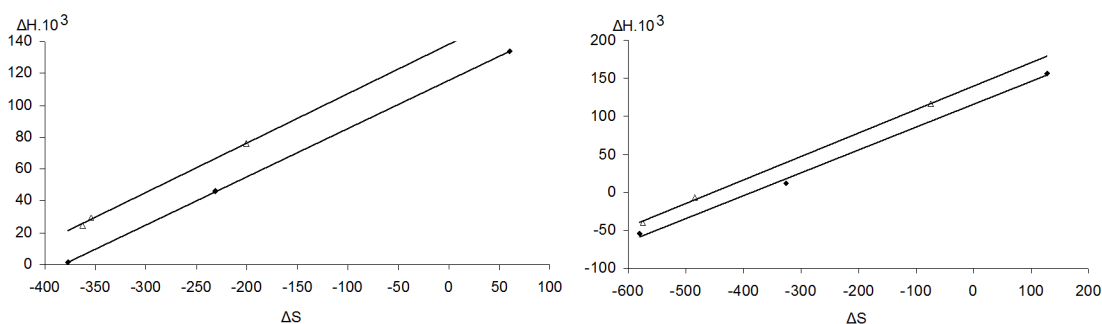
$$J \log [S] - \log K = Y \quad (22)$$

[S] and  $\Delta G$  represent the solvent concentration and the free energy, respectively. The data are collected in Table 9 and 10.  $Y$  is plotted against  $X$  (Figure 4a,b). Trail values of  $J = 1, 2, 3, 4, \dots$  are used to find values of  $W$  for the gradients of  $Y$  vs.  $X$ . The data obtained may throw light on the role of aquation and solvation during the dissociation.



**Table 8.** Thermodynamic parameters of ionization of the compounds in different percentages of ethanol+water and dioxane+water\*.

% of Solvents	Compound	pK				$\Delta G$ Kcal mol <sup>-1</sup>	$\Delta H$ Kcal mol <sup>-1</sup>	$\Delta S$
		25 °C	30 °C	35 °C	40 °C			
25% Ethanol+water	DNR	7.24 (10.87)	7.49 (10.83)	6.93 (10.60)	6.97 (10.65)	115053.07 135077.89	46129.58 29409.69	-231.17 -354.41
	AHPBA	10.41	10.47	10.40	10.42	67208.02	-2534.79	-233.92
	AHPA	10.38	10.36	10.32	10.42	67225.25	-2364.90	-233.41
	NBDTD	10.78	10.84	9.94	10.51	134540.95	59191.69	-252.72
	APP	10.87	10.75	10.40	9.44	136170.50	162353.66	87.82
50% Ethanol+water	DNR	7.06 (10.34)	7.09 (10.41)	7.30 (10.65)	6.95 (10.00)	113636.63 132749.86	1263.04 24581.91	-376.90 -362.80
	AHPBA	6.16 (10.92)	5.82 (10.13)	5.68 (9.72)	---	68526.14 67107.23	-8690.47 -11389.60	-258.99 -263.28
	AHPA	---	10.49	10.23	10.11	67151.05	-5394.61	-243.32
	AHPBAEE	10.06	9.81	9.76	9.09	67279.21	-7256.93	-250.00
	NBDTD	10.59	11.07	10.86	10.81	134444.61	-19168.73	-515.22
	APP	11.15	11.06	10.97	10.41	137206.03	79522.65	-193.47
75% Ethanol+water	DNR	8.06 (11.12)	6.02 (11.17)	7.17 (9.30)	6.42 (11.03)	115803.47 135734.05	133817.67 75923.93	60.42 -200.61
	NBDTD	11.58	11.45	11.25	11.25	139020.56	40147.34	-331.62
	APP	11.56	11.43	11.24	11.04	139131.41	60042.17	-256.27
25% Dioxane+water	DNR	6.46 (10.00)	6.02 (10.48)	6.23 (10.44)	6.26 (10.36)	109000.34 131007.77	12018.46 -40292.96	-325.28 -574.55
	DNRC	6.39 (8.26)	5.6 (8.17)	5.99 (8.18)	6.13 (8.21)	107790.14 119975.21	12534.83 2663.88	-319.49 -393.46
	AHPBA	7.61 (10.60)	6.24 (10.12)	5.94 (9.22)	5.47 (9.19)	68078.38 67175.21	-18683.26 -10594.75	-291.00 -260.84
	AHPBAEE	10.48	10.63	10.55	10.35	67174.64	-3159.54	-235.90
	NBDTD	10.97	10.80	10.74	10.19	136021.95	83008.28	-177.81
	APP	10.91	10.91	10.65	10.43	135701.78	58130.44	-260.18
	50% Dioxane+water	DNR	8.65 (11.65)	6.39 (10.95)	7.51 (10.65)	6.81 (10.65)	18768.68 138539.34	156710.31 116356.02
DNRC		7.76 (8.91)	6.56 (8.43)	6.58 (8.14)	6.72 (8.26)	115153.74 123120.34	109994.84 78330.95	-17.30 -150.23
AHPBA		7.56 (10.07)	6.67 (9.55)	6.59 (9.50)	6.52 (9.40)	68087.47 67326.76	-9618.31 -5787.92	-260.63 -245.23
AHPA		-----	8.49	8.26	8.78	67797.70	137.11	-226.93
AHPBAEE		9.20	9.24	9.24	9.35	67521.99	-1728.29	-232.27
NBDTD		11.34	11.23	11.17	11.03	137759.59	32869.52	-351.80
APP		11.37	11.30	11.21	10.91	138196.42	49768.46	-296.59
75% Dioxane+water	DNR	8.15 (11.51)	7.83 (10.98)	8.45 (11.54)	---	118652.70 137692.83	-54342.39 -6807.84	-580.23 -484.66
	NBDTD	12.11	11.75	11.87	11.71	141653.34	36380.14	-353.09
	APP	12.11	12.01	11.08	11.44	142164.63	106365.82	-120.07

\* Values between brackets are pK<sub>2</sub>.**Figure 3.**  $\Delta H$ - $\Delta S$  relationship for pK's ( $\bullet$  pK<sub>1</sub>,  $\Delta$  pK<sub>2</sub>) of dinitrosoresorcinol (DNR) in presence of different percentages mol l<sup>-1</sup> of ethanol-water and dioxane-water media at 25°C

### 3.3. Distribution of species

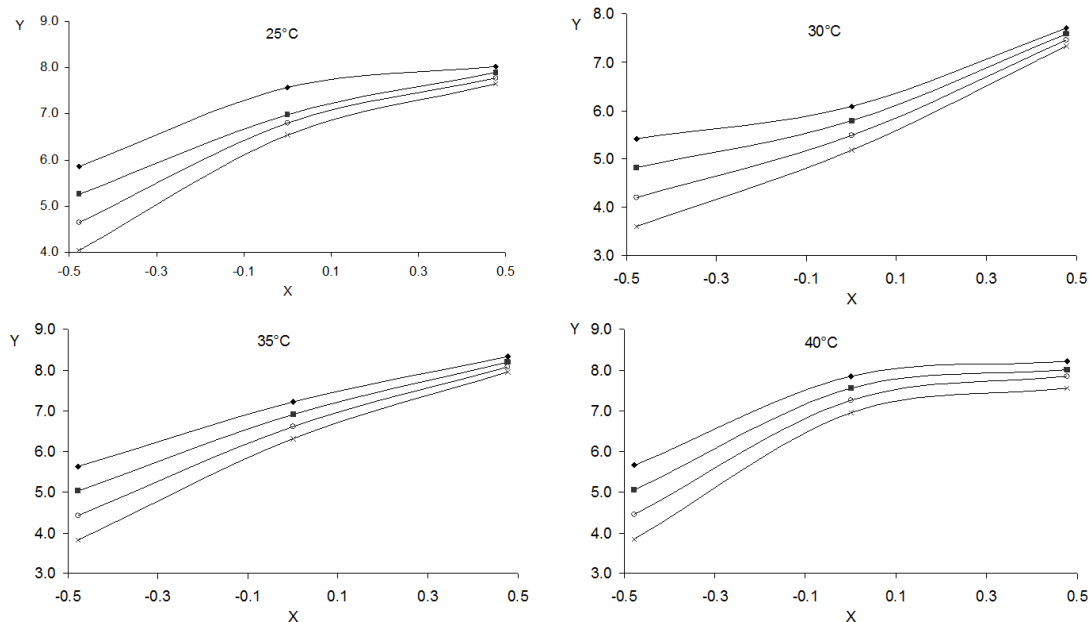
Different magnitudes of the formation constants of the complexes are manifested in different concentrations of the complex species. The concentration distribution of various (DNR, DNRC, AHPBA, AHPA, AHPBAEE, NBDTD and APP) and their complex species in solution as a function of pH are calculated and plotted using SPE and SPEPLOT computer programs [57]. Examples are given in Figures 5, 6.

From the plotting of the DNR species fraction and the pH in different % dioxane, depending on the pK values, one can extract the following points:

- 1- The curves start with high % of [H<sub>2</sub>L] species which decreased with increasing pH with appearance of [HL<sup>-</sup>] species at pH around 6.5. The concentration of both H<sub>2</sub>L and [HL<sup>-</sup>] seems to be the same i.e. each with 0.5 fraction, with increasing pH the [HL<sup>-</sup>] predominates till reach a maximum of 0.98 fraction at pH = 8. At pH > 8 the species [HL<sup>-</sup>] starts to decrease with increasing [L<sup>2-</sup>] species and at pH = 11 the [L<sup>2-</sup>] species is predominate.

**Table 9.** X-Y data for the ligands in variable contents of ethanol+water and dioxane+water media at different temperatures.

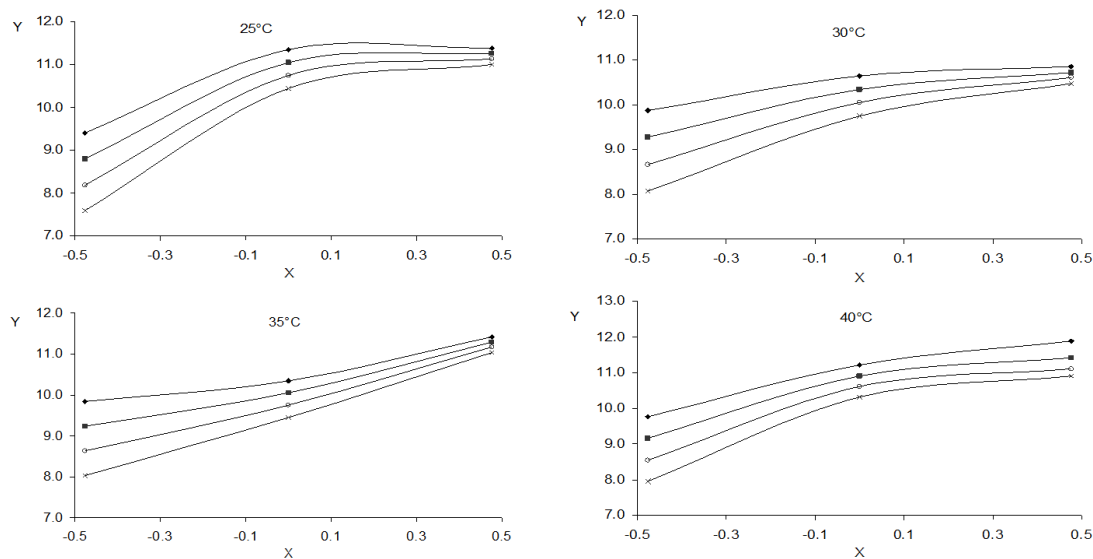
Compound	[s],%	-log[s]	-X	Y at 25 °C				Y at 30 °C			
				J=1	J=2	J=3	J=4	J=1	J=2	J=3	J=4
DNR Ethanol+water	25	0.6021	-0.477	6.64 (10.27)	6.04 (9.67)	5.43 (9.06)	4.84 (8.46)	6.89 (10.23)	6.29 (9.63)	5.69 (9.02)	5.08 (8.42)
	50	0.301	0	6.76 (10.04)	6.46 (9.74)	6.16 (9.44)	5.86 (9.14)	6.79 (10.11)	6.49 (9.81)	6.19 (9.51)	5.89 (9.21)
	75	0.1249	0.477	7.94 (10.99)	7.81 (10.87)	7.69 (10.75)	7.56 (10.62)	7.90 (11.05)	7.77 (10.92)	7.65 (10.80)	7.52 (10.67)
DNR Dioxane+water	25	0.6021	-0.477	5.86 (9.40)	5.26 (8.80)	4.65 (8.19)	4.05 (7.59)	5.42 (9.88)	4.82 (9.28)	4.21 (8.67)	3.61 (8.07)
	50	0.301	0	8.35 (11.35)	8.05 (11.05)	7.75 (10.75)	7.45 (10.45)	6.09 (10.65)	5.79 (10.35)	5.49 (10.05)	5.19 (9.75)
	75	0.1249	0.477	8.03 (11.39)	7.90 (11.26)	7.78 (11.14)	7.65 (11.01)	7.71 (10.86)	7.58 (10.73)	7.46 (10.61)	7.33 (10.48)
DNRC Dioxane+water	25	0.6021	-0.477	5.79 (7.66)	5.19 (7.06)	4.58 (6.45)	3.98 (5.85)	5.00 (7.57)	4.40 (6.97)	3.97 (6.36)	3.19 (5.76)
	50	0.301	0	7.46 (8.61)	7.16 (8.31)	6.86 (8.01)	6.56 (7.71)	6.26 (8.13)	5.96 (7.83)	5.66 (7.53)	5.36 (7.23)
AHPBA Ethanol+water	25	0.6021	-0.477	9.81 (10.62)	9.21 (10.32)	8.60 (10.02)	8.00 (9.72)	9.87 (9.83)	9.27 (9.53)	8.66 (9.23)	8.06 (8.93)
	50	0.301	0	5.86 (10.62)	5.5 (10.32)	5.26 (10.02)	4.96 (9.72)	5.52 (9.83)	5.22 (9.53)	4.92 (9.23)	4.62 (8.93)
	75	0.1249	0.477	11.11 (10.98)	10.98 (10.86)	10.86 (10.74)	10.73 (10.62)	11.31 (11.18)	11.18 (11.06)	11.06 (10.94)	10.93 (10.81)
AHPBA Dioxane+water	25	0.6021	-0.477	7.01 (10.00)	6.41 (9.40)	5.80 (8.79)	5.20 (8.19)	5.64 (9.52)	5.04 (8.92)	4.43 (8.31)	3.83 (7.71)
	50	0.301	0	7.26 (9.77)	6.96 (9.47)	6.69 (9.17)	6.36 (8.87)	6.37 (9.25)	6.07 (8.95)	5.77 (8.65)	5.47 (8.35)
AHPA Ethanol+water	25	0.6021	-0.477	9.78 (10.62)	9.18 (10.32)	8.57 (10.02)	7.97 (9.72)	9.76 (9.83)	9.16 (9.53)	8.55 (9.23)	7.95 (8.93)
	50	0.301	0	--- (10.62)	--- (10.32)	--- (10.02)	--- (9.72)	10.19 (9.83)	9.89 (9.53)	9.59 (9.23)	9.29 (8.93)
	75	0.1249	0.477	10.40 (10.99)	10.27 (10.87)	10.15 (10.75)	10.02 (10.62)	10.78 (11.05)	10.65 (10.92)	10.53 (10.80)	10.40 (10.67)
AHPBAEE Dioxane+water	25	0.6021	-0.477	9.88 (10.62)	9.28 (10.32)	8.67 (10.02)	8.07 (9.72)	10.03 (9.83)	9.43 (9.53)	8.82 (9.23)	8.22 (8.93)
	50	0.301	0	8.90 (10.62)	8.60 (10.32)	8.30 (10.02)	8.00 (9.72)	8.94 (9.83)	8.64 (9.53)	8.34 (9.23)	8.04 (8.93)
NBDTD Ethanol+water	25	0.6021	-0.477	10.18 (10.62)	9.58 (10.32)	8.97 (10.02)	8.37 (9.72)	10.24 (9.83)	9.64 (9.53)	9.03 (9.23)	8.43 (8.93)
	50	0.301	0	10.29 (10.62)	9.99 (10.32)	9.69 (10.02)	9.39 (9.72)	10.77 (9.83)	10.47 (9.53)	10.17 (9.23)	9.87 (8.93)
	75	0.1249	0.477	11.46 (10.99)	11.33 (10.87)	11.21 (10.75)	11.08 (10.62)	11.33 (11.05)	11.20 (10.92)	11.08 (10.80)	10.95 (10.67)
NBDTD Dioxane+water	25	0.6021	-0.477	10.37 (10.62)	9.77 (10.32)	9.16 (10.02)	8.56 (9.72)	10.20 (9.83)	9.60 (9.53)	8.99 (9.23)	8.39 (8.93)
	50	0.301	0	11.04 (10.62)	10.74 (10.32)	10.44 (10.02)	10.14 (9.72)	10.93 (9.83)	10.63 (9.53)	10.33 (9.23)	10.03 (8.93)
	75	0.1249	0.477	11.99 (10.99)	11.86 (10.87)	11.74 (10.75)	11.61 (10.62)	11.63 (11.05)	11.50 (10.92)	11.38 (10.80)	11.25 (10.67)
APP Ethanol+water	25	0.6021	-0.477	10.27 (10.62)	9.67 (10.32)	9.06 (10.02)	8.46 (9.72)	10.15 (9.83)	9.55 (9.53)	8.94 (9.23)	8.34 (8.93)
	50	0.301	0	10.85 (10.62)	10.55 (10.32)	10.25 (10.02)	9.95 (9.72)	10.76 (9.83)	10.46 (9.53)	10.16 (9.23)	9.86 (8.93)
	75	0.1249	0.477	11.44 (10.99)	11.31 (10.87)	11.19 (10.75)	11.06 (10.62)	11.31 (11.05)	11.18 (10.92)	11.06 (10.80)	11.93 (10.67)
APP Dioxane+water	25	0.6021	-0.477	10.31 (10.62)	9.71 (10.32)	9.10 (10.02)	8.50 (9.72)	10.31 (9.83)	9.71 (9.53)	9.10 (9.23)	8.50 (8.93)
	50	0.301	0	11.07 (10.62)	10.77 (10.32)	10.47 (10.02)	10.17 (9.72)	11.00 (9.83)	10.70 (9.53)	10.40 (9.23)	10.10 (8.93)
	75	0.1249	0.477	11.99 (10.99)	11.86 (10.87)	11.74 (10.75)	11.61 (10.62)	11.89 (11.05)	11.76 (10.92)	11.64 (10.80)	11.51 (10.67)

\* Values between brackets are  $pK_2$ .**Figure 4a.** X-Y relationship for  $pK_1$  of dinitroso resorcinol (DNR) in presence of different percentages of dioxane+water at different temperatures

◆ j=1    ■ j=2    ○ j=3    × j=4

**Table 10.** X-Y data for the ligands in variable contents of ethanol+water and dioxane+water media at different temperatures.

Compound	[s],%	-log[s]	-X	Y at 35 °C				Y at 40 °C			
				J=1	J=2	J=3	J=4	J=1	J=2	J=3	J=4
DNR Ethanol+water	25	0.6021	-0.477	6.33 (9.99)	5.73 (9.40)	5.12 (8.79)	4.52 (8.19)	6.37 (10.05)	5.77 (9.45)	5.16 (8.84)	4.56 (8.24)
	50	0.301	0	7.00 (10.35)	6.70 (10.05)	6.40 (9.75)	6.10 (9.45)	6.65 (9.70)	6.35 (9.40)	6.05 (9.10)	5.75 (8.80)
	75	0.1249	0.477	7.04 (9.18)	6.92 (9.05)	6.8 (8.93)	6.67 (8.80)	6.30 (10.91)	6.17 (10.78)	6.05 (10.66)	5.92 (10.53)
DNR Dioxane+water	25	0.6021	-0.477	5.63 (9.84)	5.03 (9.24)	4.42 (8.63)	3.82 (8.03)	5.66 (9.76)	5.06 (9.16)	4.45 (8.55)	3.85 (7.95)
	50	0.301	0	7.21 (10.35)	6.91 (10.05)	6.61 (9.75)	6.31 (9.45)	7.85 (11.21)	7.55 (10.91)	7.25 (10.61)	6.95 (10.31)
	75	0.1249	0.477	8.33 (11.42)	8.24 (11.29)	8.08 (11.17)	7.95 (11.04)	-----	-----	-----	-----
DNRC Dioxane+water	25	0.6021	-0.477	5.39 (7.58)	4.79 (6.98)	4.18 (6.37)	3.58 (5.77)	5.53 (7.61)	4.93 (7.01)	4.32 (6.40)	3.72 (5.80)
	50	0.301	0	6.26 (7.84)	5.96 (7.54)	5.66 (7.24)	5.36 (6.94)	6.42 (7.96)	6.12 (7.66)	5.82 (7.36)	5.52 (7.06)
AHPBA Ethanol+water	25	0.6021	-0.477	9.80	9.20	8.59	7.99	9.82	9.22	8.61	8.01
	50	0.301	0	5.38 (9.42)	5.08 (9.12)	4.78 (8.82)	4.48 (8.52)	-----	-----	-----	-----
	75	0.1249	0.477	-----	-----	-----	-----	-----	-----	-----	-----
AHPBA Dioxane+water	25	0.6021	-0.477	5.34 (8.62)	4.74 (8.02)	4.13 (7.41)	3.53 (6.81)	4.87 (8.59)	4.27 (7.99)	3.66 (7.38)	3.06 (6.78)
	50	0.301	0	6.29 (9.20)	5.99 (8.90)	5.69 (8.60)	5.39 (8.30)	6.22 (9.10)	5.92 (8.80)	5.62 (8.50)	5.32 (8.20)
AHPA Ethanol+water	25	0.6021	-0.477	9.36	9.03	8.42	7.82	9.82	9.22	8.61	8.01
	50	0.301	0	9.93	9.63	9.33	9.03	9.81	9.51	9.21	8.91
	75	0.1249	0.477	-----	-----	-----	-----	-----	-----	-----	-----
AHPBAEE Dioxane+water	25	0.6021	-0.477	9.95	9.35	8.74	8.14	9.75	9.15	8.54	7.94
	50	0.301	0	8.94	8.64	8.34	8.04	9.05	8.75	9.45	9.15
NBDTD Ethanol+water	25	0.6021	-0.477	9.34	8.74	8.13	7.53	9.91	9.31	8.70	8.10
	50	0.301	0	10.56	10.26	9.96	9.66	10.51	10.21	9.91	9.61
	75	0.1249	0.477	11.13	11.00	10.88	10.75	11.13	11.00	10.88	10.75
NBDTD Dioxane+water	25	0.6021	-0.477	10.14	9.54	8.93	8.33	9.59	8.99	8.38	7.78
	50	0.301	0	10.87	10.57	10.27	9.97	10.73	10.43	10.13	9.83
	75	0.1249	0.477	11.75	11.62	11.50	11.37	11.59	11.46	11.34	11.21
APP Ethanol+water	25	0.6021	-0.477	9.80	9.20	8.59	7.99	8.84	8.24	7.63	7.03
	50	0.301	0	10.67	10.37	10.07	9.77	10.11	9.81	9.51	9.21
	75	0.1249	0.477	11.16	10.99	10.87	10.74	10.92	10.79	10.67	10.54
APP Dioxane+water	25	0.6021	-0.477	10.05	9.45	8.84	8.24	9.83	9.23	8.62	8.02
	50	0.301	0	10.91	10.61	10.31	10.01	10.61	10.31	10.01	9.71
	75	0.1249	0.477	10.96	10.83	10.71	10.58	11.29	11.16	11.04	10.91

\* Values between brackets are pK<sub>a</sub>.

(b)

**Figure 4b.** X-Y relationship for pK<sub>2</sub> of dinitroso resorinol (DNR) in presence of different percentages of dioxane+water at different temperatures

◆ j=1    ■ j=2    ○ j=3    × j=4

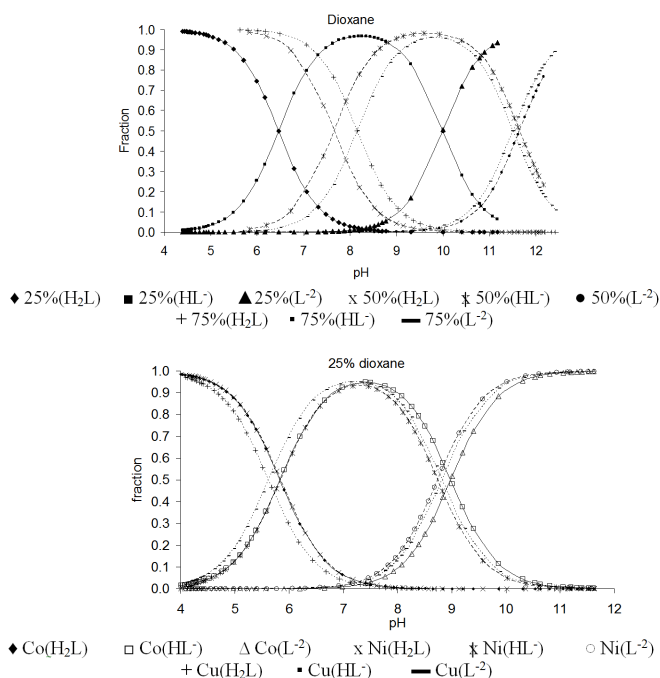


Figure 5. Species distribution diagram of the DNR and its complex

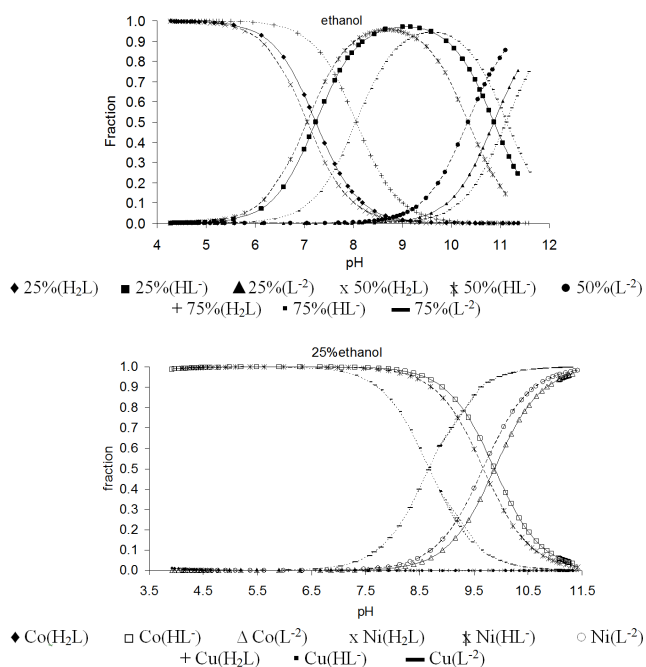


Figure 6. Species distribution diagram of the DNR and its complex.

2- By increasing the % dioxane from 25% to 50% and then to 75% gave the same trend but the curves shifted to a higher pH. This leads to the fact that the pK values increase with increasing dioxane %, and this may be due to the dielectric properties of the dioxane that retard the dissociation of the DNR acid species.

3- The study of the Co, Ni and Cu complexes gave the same trend as the ligand, where on increasing pH the MH<sub>2</sub>L species decrease till it reaches a minimum at pH 7.5 while the MHL<sup>-</sup> species starts to increase starting from pH = 4.1 till reaching a maximum at 7.5 then decreases with increasing ML<sup>-2</sup> species. The ML<sup>-2</sup> species predominate at pH > 10. The difference between the complexes and the

free ligand may be attributed to the electrophilic nature of the metal ion in the complexes. These metal ions attract electrons from the organic ligand and make its dissociation difficult. One can arrange the electrophilic nature as  $\text{Co}^{+2} > \text{Cu}^{+2} > \text{Ni}^{+2}$ , Figure 5.

- 4- In case of ethanol, DNR gave the same trend, Figure 6, where the species  $\text{H}_2\text{L}$ ,  $\text{HL}^-$  and  $\text{L}^{2-}$  are present in the ligand curve but in case of complexes only  $\text{M}(\text{H}_2\text{L})$  and  $\text{MHL}^-$  species are present. This may be due to the strong attraction between the metal ion and DNR as a ligand in ethanol, where DNR dissociate one H-ion to form an acidic coordination bond, so the complex would have one pK.
- 5- The strong interaction between the metal and the ligand makes the first hydrogen is readily to dissociate at  $\text{pK}=1.99\text{-}2.03$ .

#### 4. Conclusion

The contributions of the refractive index and the dielectric constant of the solvents with the location of the peak position of the band in the vaporized state through two-parameter mathematical equation were explained using PC statistical program. It is concluded that the addition of a third solvent parameter to the two-parameter equations always gave rise to improvements in the correlation with the solvent induced spectral shifts. The correlation equation based on all solvent parameters is the best to get convenient statistical description of the relation. Multiple regression technique was used in order to evaluate  $U_{\text{(vapour)}}$ ,  $K_1$ ,  $K_2$  and the correlation coefficients. The data show strong dependence of the shift in  $\lambda_{\text{max}}$  of [DNR on  $X_1$ , DNRC on  $(X_1, X_2)$  and NBDTD on  $(X_1, X_2)$ ]. The potentiometric titration measurements indicated that  $\text{pK}_1$  (6.39 – 8.15) and  $\text{pK}_2$  (8.26 – 12.11) values are strongly affected with the % of the co-solvent. The thermodynamic parameters of dissociation of the free organic compounds were evaluated. The isokinetic temperature relationship for the plot of  $\Delta H$  versus  $\Delta S$  based on  $\text{pK}_1$  and  $\text{pK}_2$  values gave best-fit straight lines. The effects of ethanol and dioxane solvents on the behaviour of the compounds were explained from hydration and solvation views during the course of dissociation. The formation constants of the complexes were evaluated by pH-metric measurements.

#### References

- [1]. Arranz, M. P.; Lopez, G. R.; Gutierrez, V. M. D.; Godino, S. M. L.; Mareno, J. M. *Inorg. Chim. Acta* **2000**, *304*, 137-143.
- [2]. Melguizo, M.; Marchal, A.; Noguera, M.; Sanchez, A.; Low, J. N. *J. Heterocyclic Chem.* **2002**, *39*, 97-103.
- [3]. Lopez, G. R.; Arranz, M. P.; Godino, S. M. L.; Gutierrez, V. M. D.; Perez, C. A.; Cobo, D. J.; Moreno, J. M. *Inorg. Chim. Acta* **2000**, *308*, 59-64.
- [4]. Yun, J.; Choi, H. *Talanta* **2000**, *52*(5), 893-902.
- [5]. Ghaly, A. E.; Dave, D.; Budge, S.; Brooks, M. S. *Am. J. App. Sci.* **2010**, *7*, 859-877.
- [6]. Foreti, B.; Burger, N.; Hankonyi, V. *Polyhedron* **1995**, *14*, 605-609.
- [7]. Totsuka, Y.; Nishigaki, R.; Enomoto, S.; TakamuraEnya, T.; Masumura, K.; Nohmi, T.; Kawahara, N.; Sugimura, T.; Wakabayashi, K. *Chem. Res. Toxicology* **2005**, *18*(10), 1553-1562.
- [8]. Coss, A.; Cantor, K. P.; Reif, J. S.; Lynch, C. F.; Ward, M. H. *Am. J. Epidem.* **2004**, *159*, 7, 693-701.
- [9]. Kandil, S. S.; El-Hefnawy, G. B.; Bakr E. A.; Abou El-Ezz, A. Z. *Trans. Met. Chem.* **2003**, *28*, 168-175.
- [10]. Dinda, J.; Pal, S.; Ghosh, B. K.; Sinha, C.; Cheng, J.; Liao, F. L.; Lu, T. H. *J. Coord. Chem.* **2002**, *55*, 1271-1281.
- [11]. Rauth, G. K.; Dinda, J.; Jasimuddin, S.; Sinha, C. *Trans. Met. Chem.* **2003**, *28*, 88-95.
- [12]. Byabartta, P.; Pal, S.; Misra, T. K.; Sinha, C.; Liao, F. L.; Panneerselvam, K.; Lu, T. H. *J. Coord. Chem.* **2002**, *55*, 479-495.
- [13]. Pramanik, K.; Shivakumar, M.; Ghosh, P.; Chakravorty, A. *Inorg. Chem.* **2000**, *39*, 195-199.
- [14]. Shivakumar, M.; Pramanik, K.; Bhattacharyya, I.; Chakravorty, A. *Inorg. Chem.* **2000**, *39*, 4332-4338.
- [15]. Shivakumar, M.; Gangopadhyay, J.; Chakravorty, A. *Polyhedron* **2000**, *20*, 2089-2093.
- [16]. Hotze, A. C. G.; Broekhuisen, M. E. T.; Velders, A. H.; Vander Schilden, K.; Haasnoot, J. G.; Reedijk, J. *Eur. J. Inorg. Chem.* **2002**, *2*, 369-376.
- [17]. Saha, A.; Majumdar, P.; Peng, S. M.; Goswami, S. *Eur. J. Inorg. Chem.* **2000**, *12*, 2631-2639.
- [18]. Masoud, M. S.; Abou El-Enein, S. A.; Obeid, N. A. Z. *Fur Phys. Chem.* **2001**, *215*, 7, 867-881.
- [19]. Masoud, M. S.; Abou El-Enein, S. A.; Kamel, H. M. *Ind. J. Chem.* **2002**, *41A*, 297-303.
- [20]. Masoud, M. S.; Mohamed, G. B.; Abdol Razek, Y. H.; Ali, A. E.; Khiry, F. N. *Spectroscopy Lett.* **2002**, *35*, 377-413.
- [21]. Masoud, M. S.; Abou El-Enein, S. A.; Ayad, M.; Goher, A. S. *Spectrochim. Acta A* **2004**, *60*(1), 77-87.
- [22]. Masoud, M. S.; Khalil, E. A.; Hafez, A. M.; El-Husseiny, A. F. *Spectrochim. Acta A* **2005**, *61*, 989-993.
- [23]. Masoud, M. S.; El-Husseiny, A. F.; Abd El-Ghany, M. M.; Hammud, H. H. *Bull. Fac. Sci. Alex. Univ.* **2006**, *44*(1,2), 41-54.
- [24]. Masoud, M. S.; Khalil, E. A.; Ramadan, A. M. *J. Anal. & App. Pyrolysis* **2007**, *78*(1), 14-23.
- [25]. Masoud, M. S.; Khalil, E. A.; Ramadan, A. M.; Gohar, Y. M.; Sweyllam, A. *Spectrochim. Acta* **2007**, *67A*, 669-677.
- [26]. Masoud, M. S.; Abou El-Enein, S. A.; Ramadan, A. M.; Goher, A. S. *J. Anal. & App. Pyrolysis* **2008**, *81*, 45-51.
- [27]. Van V. L. G.; Hass, C. G. *J. Am. Chem. Soc.* **1953**, *75*, 451-455.
- [28]. Reichardt, C. *Chem. Rev.* **1994**, *94*, 2319-2358.
- [29]. Hilliard, L. J.; Foulk, D. S.; Gold, H. S. *Anal. Chim. Acta* **1981**, *133*, 319-327.
- [30]. Masoud, M. S.; Hasanein, A. A.; Heiba, A. M. *Spectrosc. Lett.* **1984**, *17*, 441-453.
- [31]. Masoud, M. S.; Khalil, E. A. Polish J. Chem. **1991**, *65*, 933-943.
- [32]. Masoud, M. S.; Hasanein, A. A.; Ghonaim, A. K.; Khalil, E. A.; Mahmoud, A. A. Z. *Fur Phys. Chem. Bd.* **1999**, *209S*, 223-238.
- [33]. Masoud, M. S.; Ali, A. E.; Shaker, M. A.; Abdul Ghani, M. *Spectrochim. Acta* **2004**, *60A*, 3155-3159.
- [34]. Kirkwood, J. G. *J. Chem. Phys.* **1934**, *2*, 351-361.
- [35]. David, J. G.; Hallam, H. E. *Spectrochim. Acta* **1967**, *23 A*, 593-603.
- [36]. McRae, E. G. *J. Phys. Chem.* **1957**, *61*, 562-572.
- [37]. Fowler, F. W.; Katritzky, A. R.; Rutherford, R. J. D. *J. Chem. Soc. (B)* **1971**, 460-469.
- [38]. Hantzsch, A. *Ber. Dtsch. Chem. Ges.* **1922**, *55*, 953-979.
- [39]. Franck, J. J. *Trans. Faraday Soc.* **1926**, *21*, 536-542.
- [40]. Dearden, J. C.; Forbes, W. F. *Can. J. Chem.* **1960**, *38*(6), 896-910.
- [41]. Masoud, M. S.; Ali, G. Y. *J. Chin. Chem. Soc. (Taipei)* **1981**, *28*, 103-106.
- [42]. Masoud, M. S.; Hammad, H. H. *Spectrochim. Acta* **2001**, *57 A*, 977-984.
- [43]. Masoud, M. S.; Ali, A. E.; Shaker, M. A.; Abdul Ghani, M. *Spectrochim. Acta* **2005**, *61A*, 3102-3107.
- [44]. Kim, J. J.; Funabiki, K.; Muramatsu, H.; Shibata, K.; Kim, S. H.; Shiozaki, H.; Hartmann, H.; Matsui, M. *J. Chem. Soc. Perkin Trans.* **2001**, *2*, 379-387.
- [45]. Monahan, A. R.; De Luca, A. F.; Ward, A. T. *J. Org. Chem.* **1971**, *36*, 3838-3842.
- [46]. Ramaekers, R.; Dehaen, W.; Adamowicz, L.; Maes, G. J. *Phys. Chem. A* **2003**, *107*, 1710-1719.
- [47]. Patrick, R. A.; Svehla, G. *Anal. Chim. Acta* **1977**, *88*, 363-370.
- [48]. Masoud, M. S.; Kaddah, A. M.; Khalil, A. M.; Tawfik, N. I. *Indian J. Chem.* **1979**, *17A*, 502-504.
- [49]. Jahagirdar, D. V.; Khanolkar, D. D. *J. Inorg. Nucl. Chem.* **1973**, *35*, 921-930.
- [50]. Charberk, S.; Martell, A. E. *J. Am. Chem. Soc.* **1952**, *74*, 5052-5056.
- [51]. Khalil, E. A.; Masoud, M. S.; El-Marghany, A. M. *Pak. J. Sci. Ind. Res.* **1993**, *36*, 68-73.
- [52]. Mui, K.; McBryde, W.; Neiboer, E. *Can. J. Chem.* **1974**, *52*, 1821-1833.
- [53]. Kreshkov, A. P. *Talanta* **1970**, *17*, 1029-1044.
- [54]. Coetzee, J. F.; Ritchie, C. D. *Solute-Solvent Interactions*. Marcel Dekker. New York, 1969, pp. 221.
- [55]. Denison, J. T.; Ramsey, J. B. *J. Am. Chem. Soc.* **1955**, *77*, 2615-2621.
- [56]. Yeh, S. J.; Jaffe, H. H. *J. Am. Chem. Soc.* **1959**, *81*, 3279-3283.
- [57]. Martell, A. E.; Mutekaities, R. J. *Determination and Use of Stability Constants*, VCH, New York, 1992.